



# RESIDUAL INDENTATION, DELAMINATION AREA AND CAI STRENGTH OF CFRP LAMINATES UNDER LOW-VELOCITY IMPACT

Hiroshi Kondo\*, Yuichiro Aoki\*\*, Katsumi Hiraoka\* and Hiroshi Hatta\*\*

\*Tokai University, Kanagawa, Japan

\*\*Japan Aerospace Exploration Agency, Tokyo, Japan

**Keywords:** *Low-velocity impact, dent, CAI strength, Delamination*

## Abstract

*The relationships with dent and delamination size, subsequent compression after impact (CAI) strength are investigated by experiment and numerical analysis. Low-velocity impact is given to quasi-isotropic carbon fiber reinforced plastic (CFRP) laminates by various shapes of steel impactor and dent depth and shape are measured by a laser displacement sensor. Non-destructive inspection (NDI) is carried out by an ultrasonic C-scanning system to observe the delamination shape. Then, compression tests are carried out by a screw-driven test machine and CAI strengths are examined. Response of CFRP laminates during impact event and shape and size of delamination depend on the impactor shape even for the same impact energy. Thus subsequent CAI strength of the impacted laminates also depends on the impactor shape. Conical and pyramid shape impactors give more significant impact damage and the reduction of CAI strength than hemispherical and flat shape impactors.*

## 1 Introduction

Recently, composite material is used for aircraft structures extensively to reduce the weight with high strength and stiffness. In aircraft applications the composites have to survive low energy impacts from dropped tools during maintenance and hail-fall during aircraft parking etc. The conventional structures made of composite laminates, however, are vulnerable to impact damages because of there is no reinforcement through-the-thickness direction. These damages (i.e. delamination and transverse crack) are barely visible from outside but cause a severe reduction of compressive strength of the structure. That phenomena is known as CAI problem

and significant concern in the aerospace research field because the design loads of aircraft composite structures are often limited by that degraded compressive strength. Therefore, it is important to understand the mechanism of damage accumulation in composite laminates subjected to low-velocity impact and CAI behavior.

Many researches on CAI phenomenon have been conducted by experiments [e.g. 1-5]. Most experiments focus on relationship between delamination area and CAI strength. On the other hand, visible indentation remains on the surface of the material after impact which is generally called "dent". The dent is a sort of permanent local plastic deformation of the resin caused by impact load. The size of local deformation depends on the impactor shape and may have correlation with delamination growth. A few experimental studies have been made on the effect of impactor shape on the impact response [6] and damage mechanism [7]. The numerical analysis for impact event of CFRP structure has focused on contact behavior based on a contact law [8-10]. Few researches, however, have been reported on the relationship between dent and CAI strength as well as delamination area. It must be useful if the degraded strength can be predicted by visual inspection of dent without using NDI equipment during the aircraft maintenance. Therefore, the research on dent will provide a new insight into the CAI problem.

This study focuses on the dent as a characteristic sign of impact. The relationships with dent, delamination size and CAI strength are investigated by experiment. In addition, the effect of impactor shape on impact response is also considered. Correlation with the local plastic deformation and delamination growth is analyzed by finite element analysis to clarify the effect of dent on delamination

growth. The finite element model based on a virtual crack closure technique and elastic-plastic material model is used to simulate the delamination growth and dent creation under low-velocity impact.

## 2 Experimental

### 2.1 Materials and Specimens

The material used in this study was T800S/3900-2B, high strength carbon fiber and toughened epoxy resin prepreg system, supplied by TORAY Co., ltd. This prepreg is toughened by thermoplastic particles distributed on the prepreg surface. The panels were cured in a hot-press machine following a recommended cure cycle. The stacking sequence was  $[45/0/-45/90]_{4s}$ , quasi-isotropic 32 ply laminates, with a nominal thickness of 5.9 mm. An average fiber volume fraction of cured laminates was 56.2 %. Specimens, size of 150 mm  $\times$  100 mm, were cut from the parent panels by a diamond cutting wheel in reference to the Suppliers of Advanced Composite Materials Association Standard for CAI test, SACMA SRM 2R-94. All the specimens were visually inspected for any defects such as thickness variations which could lead to stress concentrations and affect the experimental data.

### 2.2 Impact test

Impact was given to the center of the specimen by the drop-weight impact test machine, INSTRON 9250HV. A rebound brake is attached to the test machine to prevent multiple impacts on the specimen by the impactor. Seven different shapes of impactors were used for the test. The impactor shapes were mainly classified to hemispherical, flat and conical and pyramid. The detail of the impactors is summarized in Table 1 and the overview of impactor is shown as Fig. 1. The impact tests were conducted under different impact energies ranged from 1.0 to

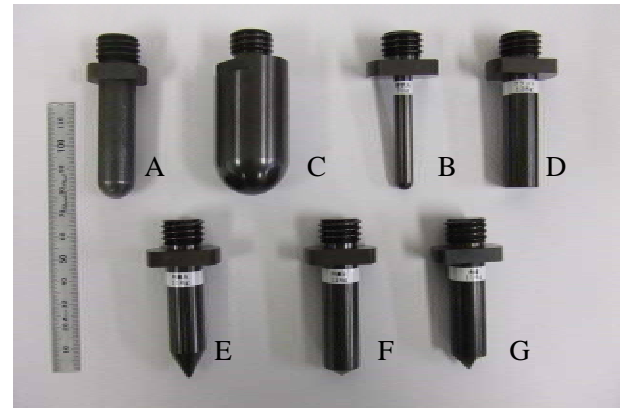


Fig. 1 Overview of impactors

10.5 J/mm (i.e. from 5.9J to 62.0 J), where impactor mass and height were adjusted. The impact velocity was ranged from 1.43 to 4.06 m/sec. Impact load, velocity and deflection of specimen were measured by an instrumented impactor (Dynatup) and consider the behavior of impacted specimen. The specimens were clamped at four points by toggle rubbers shown as Fig. 2

### 2.3 Damage inspection

After the impact test, indentation depth and shape on the specimen surface were measured by three-dimensional measurement system. An overview of the measurement system is illustrated in Fig. 3. There is two axes (X, Y) stage under the fixed laser displacement sensor (KEYENCE LK-080). Both X and Y data can be measured by 0.1 mm pitch and the minimum resolution of the sensor is 30 $\mu$ m. After dent measurement, non destructive inspection (NDI) was performed by using an ultrasonic C-Scanning system (Krautkramer SDS5400R) with a 5 MHz

	Tip shape	Diameter (mm)
Type A	Hemisphere	15.9
Type B	Hemisphere	7.95
Type C	Hemisphere	31.8
Type D	Flat	15.9
Type E	Conical (60°)	15.9
Type F	Conical (120°)	15.9
Type G	Pyramid (90°)	15.9

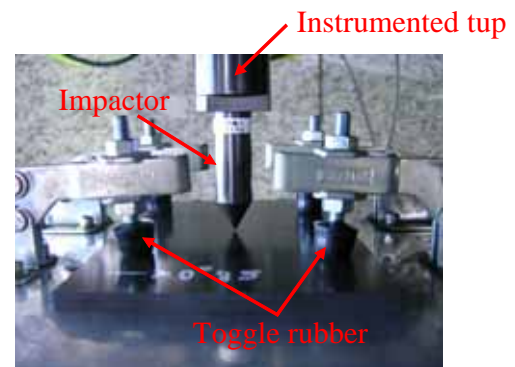


Fig. 2 Impact test fixture

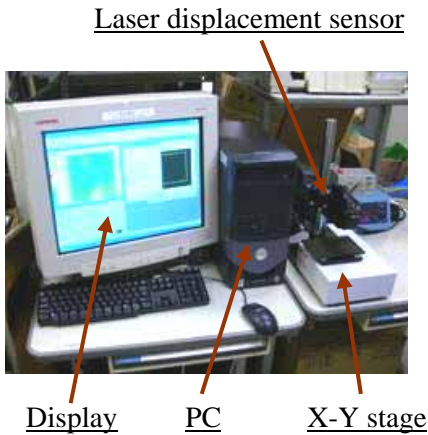


Fig. 3 Three-dimensional measurement system

transducer in pulsed-echo mode to examine the delamination area, size and shapes. The delamination area is defined by the projection area of the whole delamination obtained by C-scan image. After ultrasonic inspection, some of the specimens were cut into slices by diamond fine saw at their center and the through-the-thickness delamination pattern of the sliced specimens was observed by a microscope.

#### 2.4 Compression test

Compression after impact tests were carried out by a screw-driven test machine, INSTRON 1182, under displacement control with a crosshead speed of 1.0 mm/min. CAI test fixture described in the SACMA SRM 2R-94 are used shown as Fig.4. Top and bottom edges are fixed and out-of-plane displacement at side edges are simply supported by knife edge fixtures. The compressive load, displacement and strains are measured by KYOWA



Fig. 4 Test apparatus for compression test after impact

PCD-300 data logger with a sampling rate of 10 Hz during the test.

### 3 Results and Discussion

#### 3.1 Effect of impactor shape on impact behavior

Typical load-time histories produced by the hemispherical, flat, conical (60°) and pyramid impactors at impact energy of 6.7 J/mm are shown in Fig. 5. The histories show characteristic features distinguished by the impactor shape. The flat impactor produced the highest contact force and shortest contact duration whereas the conical impactor produced the lowest contact force and longest contact duration. The smaller contact forces produced by the conical and pyramid impactors are attributed to the fiber breakage caused by the sharp-pointed impactor tip. That leads to local penetration and results in friction between the impactor and specimen. Therefore, the contact durations increase in cases of conical and pyramid impactors.

#### 3.2 Effect of impactor shape on impact-induced damage

The results of ultrasonic C-scan from the back surface for the specimen impacted by various impactor shapes at impact energy of 6.7 J/mm are shown in Fig. 6. The overall shape of the whole delamination area is circular. The delamination size near the back surface tends to be larger than that near the top surface for all specimens except for the specimen impacted by flat shape impactor. The flat shape impactor caused a large size delamination only near the middle layer.

Damage on the front surface induced by various

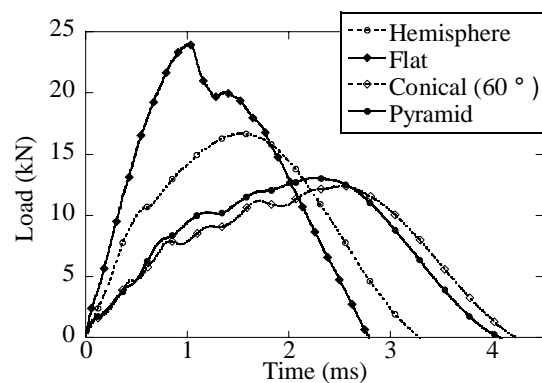


Fig. 5 Impact load histories obtained by different impactors

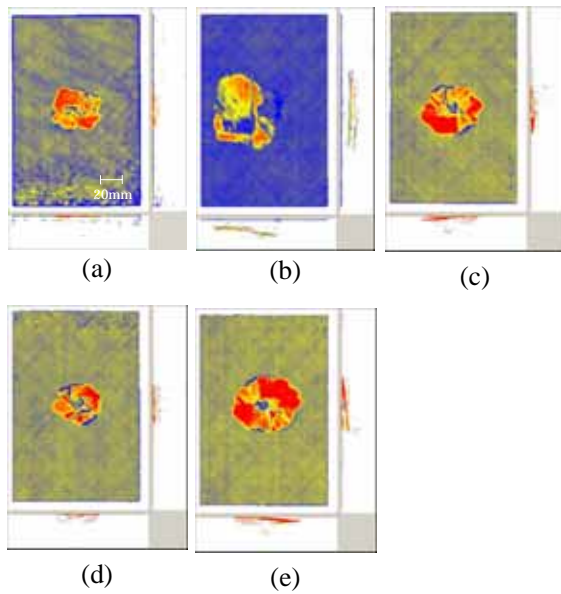


Fig. 6 Ultrasonic C-scan images for the impacted specimen by various impactor shapes: (a) hemispherical (d=15.9mm), (b) flat, (c) conical (60°), (d) conical (120°), (e) pyramid

impactor shapes is shown in Fig. 7. A difference can be seen in the patterns of surface damage. The hemispherical impactor produced residual indentation and matrix cracking of the surface. Only the contour of impactor tip was remained by flat shape impactor. Fiber breakage and small penetration were observed by conical and pyramid impactors.

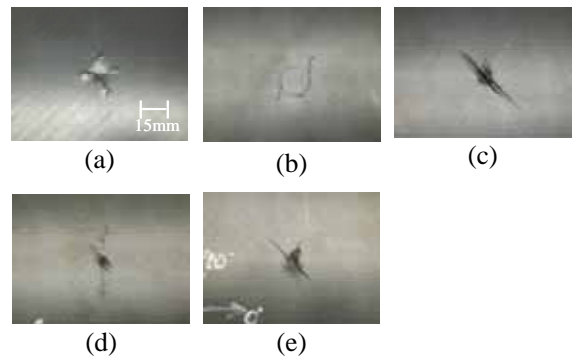


Fig. 7 Indentations for the impacted specimen by various impactor shapes: (a) hemispherical (d=15.9mm), (b) flat, (c) conical (60°), (d) conical (120°), (e) pyramid



Fig. 8 Cross sectional observation for the impacted specimen by (a) hemispherical, (b) flat, (c) conical, (d) pyramid impactors

### 3.3 Cross sectional observation

Damage state under impact location of hemispherical, flat, conical (60°) and pyramid impactors at impact energy of 6.7 J/mm were observed by an optical microscope. The schematic drawing of the microphotograph was obtained by tracing the damage shown as Fig. 8. All the impactor except for the flat shape produced large delaminations near back side. The flat shape impactor caused a large size delamination only near the middle layer.

### 3.4 Summary of impactor shape effect on impact response and CAI strength

Figure 9 summaries peak contact load, delamination area and CAI strength for the specimen impacted by various impactors. In this figure, impactor with sharp tip gave low peak load, large delamination area and high CAI strength, whereas flat impactor gave high

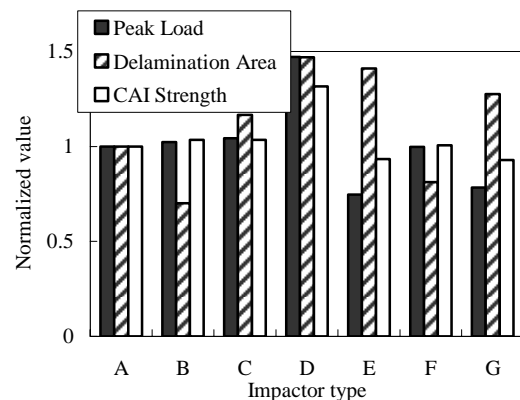


Fig. 9 Summary of impactor shape effects on peak load, delamination area and CAI strength

peak load, large delamination area and high CAI strength. Since the flat shape impactor produced the largest projection area of delamination but the



damage accumulation through-the-thickness is not so significant compared with other impactors, the CAI strength is relatively larger than other specimens.

### 3.5 Indentation depth and delamination area

The relationship between delamination area and measurable residual indentation is shown in Fig. 10. Only the hemispherical and flat shapes impactor produced the measurable indentation. The indentation depth tends to increase in the same manner up to about 0.15 mm for all hemispherical impactor. Delamination area increases rapidly after that point. The increasing ratio of indentation depth depends on the diameter of impactor because of contact behavior is different in each impactor case. From this figure, it was found that there is transition of failure modes, i.e. dent creation region at low impact energy level and delamination growth region at larger impact energy.

### 3.4 Indentation depth and CAI strength

Figure 11 shows the relationship between the indentation depth and CAI strength. The curve also can be divided into two regions, i.e. dent creation and delamination growth. The CAI strength tends to be constant when the dent depth is smaller than 0.15 mm and decrease significantly when the dent depth is larger than 0.15 mm. This result shows that there is a critical dent depth as a trigger of decreasing CAI strength and then the strength can be predicted by visual inspection of dent.

## 4 Finite Element Analysis

Correlation with the dent and delamination growth is considered by preliminary finite element analysis to clarify the mechanism of impact-induced damage. Present analysis is still preliminary stage and only the effect of permanent local plastic deformation on delamination growth was considered. A finite element analysis models of circular CFRP laminates and hemispherical indenter were modeled by axisymmetric element as shown in Fig. 12. The material was assumed to be isotropic, which is equivalent in-plane property of quasi-isotropic laminates for present CFRP. The material properties used in the analysis are shown in Table 2. To simplify the problem, static displacement was applied to the impactor instead of low-velocity impact. Local plastic deformation and delamination growth are considered in this analysis. The surface

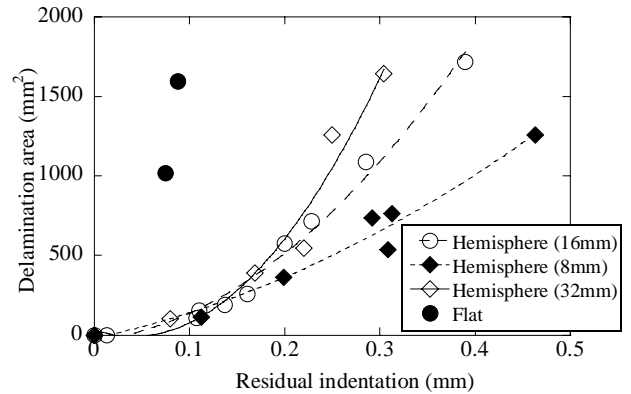


Fig. 10 Relationships between residual indentation and delamination area

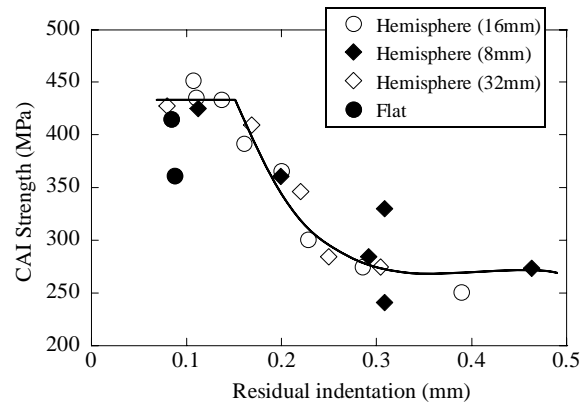


Fig. 11 Relationships between residual indentation and delamination area

layer near the indentation area was assumed to have a bi-linear elastic-plastic material property, which can simulate a dent creation after indenter contacting. The model with only elastic material property was also analyzed to compare the results with elastic-plastic model. A commercially available finite element analysis code, ABAQUS Ver.6.6, was used for the present analysis. Delamination propagation under loading was simulated by the option of VCCT for ABAQUS. A fracture criterion for delamination propagation is defined following power law based on the fracture mechanical parameters.

$$\left(\frac{G}{G_c}\right)^{am} + \left(\frac{G}{G_c}\right)^{an} + \left(\frac{G}{G_c}\right)^{ao} = 1$$

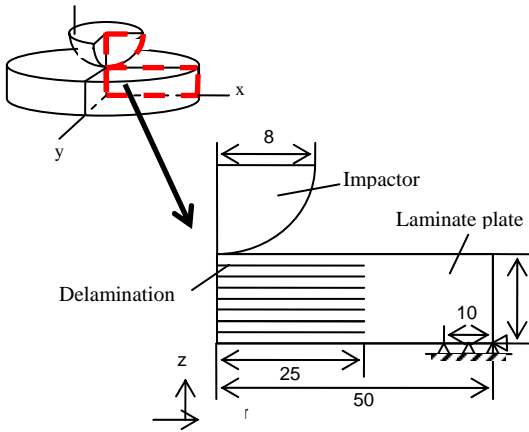


Fig. 12 Finite element analysis model

Table 2 Material properties

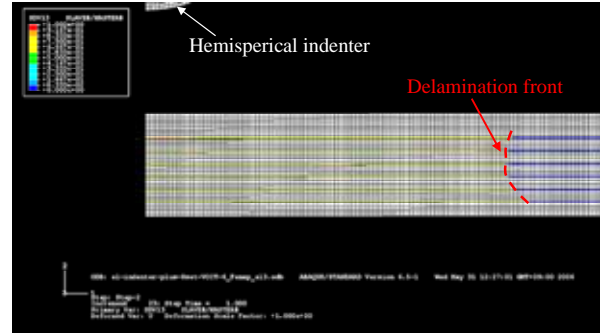
Plate Young's modulus (GPa)	8
Plate Yield stress (MPa)	30
Plate Poisson's ratio	0.3
Impactor Young's modulus (GPa)	210
Impactor Poisson's ratio	0.3

where,  $am = an = ao = 1$ , and  $G_{IC} = 0.54 \text{ kJ/m}^2$ ,  $G_{IIC} = G_{IIIC} = 1.64 \text{ kJ/m}^2$  were used in present analysis.

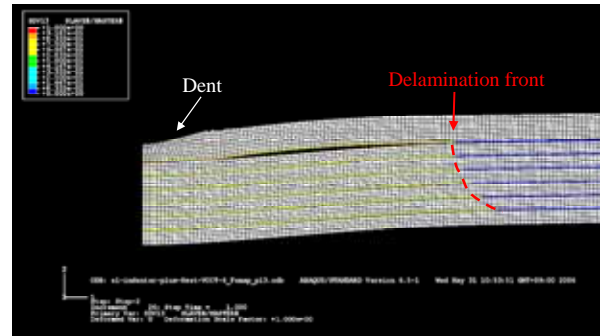
Comparison of analysis results is shown in Fig. 13. There are some differences between elastic model and elastic-plastic model. For elastic-plastic model, obvious dent remains at contacting area and delamination size is slightly smaller than elastic model. Shape of delamination through-the-thickness is also different, where the size of delamination gradually increases toward the bottom surface in elastic-plastic model whereas delamination size tends be small near the middle layer in elastic model. Therefore, the effect of permanent local deformation on delamination growth is significant. Predicted final damage shape and size depends on the local indentation.

## 5 Conclusions

The relationships with dent, delamination size and CAI strength are investigated by experiment. The effect of impactor shape on impact response is also considered. In addition, correlation with the permanent local deformation and delamination growth is analyzed by finite element analysis to clarify the effect of the dent on delamination growth.



(a) Elastic model



(b) Elastic-plastic model

Fig. 13 Analysis results after unloading

The main conclusions are as follows.

The impact histories show characteristic features distinguished by the impactor shape. The contact force and duration depends on impactor shape. Impactor with sharp tip gave low peak load, large delamination area and low CAI strength, whereas flat impactor gave high peak load, large delamination area and high CAI strength. Since the flat shape impactor produced the largest projection area of delamination but the damage accumulation through-the-thickness is not so significant compared with other impactors, the CAI strength is relatively larger than other specimens.

It was found that there is transition of failure modes, i.e. dent creation region at low impact energy level and delamination growth region at larger impact energy. This result shows that there is a critical dent depth as a trigger of decreasing CAI strength and then the strength can be predicted by visual inspection of dent.

The effect of permanent local deformation on delamination growth is significant. Predicted final damage shape and size depends on the local indentation. Therefore, the dent is one of the crucial factor associated with size and shape of impact-induced delamination.



## References

- [1] Freitas M.de., Reis L. “Failure mechanisms on composite specimens subjected to compression after impact”. *Composite Structures*, Vol. 42, pp 365-373, 1998.
- [2] T. Ishikawa, S. Sugimoto, M. Matsushima and Y. Hayashi, Some experimental findings in CAI tests of CF/PEEK and conventional CF/EPOXY at plates, *Composites Science and Technology*, 55, pp.349-362, 1995.
- [3] H-Y. T. Wu and G. S. Springer, Measurements of Matrix Cracking and Delamination Caused by Impact on Composite Plates, *J. Composites Materials*, Vol. 22, No. 6, pp.518-532, 1988.
- [4] S. P. Joshi and C. T. Sun, Impact Induced Fracture in a Laminated Composite, *J. Composites Materials*, Vol. 19, pp.51-66, 1985.
- [5] H. Y. Choi, R. J. Downs and F. K. Chang, A new approach toward understanding damage mechanisms and mechanics of laminated composites due to low-velocity impact—part I: experiments, *J. Composites Materials*, Vol. 25, pp.992-1011, 1991.
- [6] Mitrevski T., Marshall I.H., Thomson R., Jones R. and Whittingham B. “The effect of impactor shape on the impact response of composite laminates”. *Composite Structures*, Vol. 67, pp 138-148, 2005.
- [7] Zhou G., Lloyd J.C. and McGuirk J.J. “Experimental evaluation of geometric factors affecting damage mechanisms in carbon/epoxy plates”. *Composites: Part A*, Vol. 32, pp 71-84, 2001.
- [8] Christoforou P.A. “On the contact of a spherical indenter and a thin composite laminate”. *Composite Structures*, Vol. 26, 77-82, 1993.
- [9] Cairns S.D. “A Simple, Elasto-Plastic Contact Law for Composites”. *Journal of Reinforced Plastics and Composites*, Vol. 10, 423-433, 1991.
- [10] Varadi K., Nader Z., Friedrich K., Flock J. “Finite-element analysis of a polymer composite subjected to ball indentation”. *Composites Science and Technology*. Vol. 59, 271-281, 1999.